

Pushing the resolution limits: The Priddis 3C-2D survey

David C. Henley, Kevin W. Hall, Malcolm B. Bertram, and Eric V. Gallant

ABSTRACT

As improvements continue to be made in seismic acquisition equipment, particularly in the number of independent channels which can be recorded and in the manner in which field apparatus is assembled and connected in the field, we continue to press for increased spatial resolution and bandwidth of the recorded wavefield. An earlier experiment conducted near Longview in 2006 demonstrated some of the benefits of recording a 2D seismic line with closely spaced single geophones in order to properly sample not only the earth structure, but the source-generated noise, so that the latter can be properly characterized and removed. We describe here a recent survey conducted at the University of Calgary Priddis test site, in which we deployed 3-C geophones spaced 1 m apart, our most finely sampled survey to date. At this spacing, almost none of the coherent noise generated by the source, including the air wave, is aliased. We show that this fine sampling enables us to image the resulting data to very high resolution limits, both vertically and laterally.

INTRODUCTION

To most geophysicists, resolution pertains to the detail with which geological features in the earth can be seen unambiguously with reflection seismic data. Much effort has been devoted to determining survey parameters designed to sample the backscattered seismic wavefield without aliasing important details of the buried geological structure, while not increasing field costs unreasonably. Only relatively recently, however, has attention shifted to another important aspect of resolution...noise discrimination. It is still the most commonly accepted practice for seismic surveys to employ linear arrays of sensors on the surface to attenuate source-generated coherent noise by horizontal summation. Another possibility, which we and others have begun to explore, is to employ single closely spaced sensors, record each sensor, and characterize and remove the noise computationally rather than with hard-wired summation. While this method presently requires somewhat more field effort due to the increased number of electrical connections to be made in the field, we can expect this difference to vanish as technology continues its evolution.

We have shown in other work (Henley et al, 2006) that horizontal summation of geophone output is probably the least effective noise attenuation method, and that we can attain a much higher signal to noise ratio (S/N) with methods such as radial trace filtering, which capture the noises efficiently in the radial trace domain and accurately model them for subtraction from the raw data. These methods are only effective, however, when the noises are unaliased over most of their bandwidth. In our 2006 work, we showed that processing a seismic survey sampled at 2.5 m provided the cleanest, highest resolution shot gathers; and the benefits carried right through to the finished migrated section, where the lateral and vertical resolution exceeded that for the same data set processed as if it had been acquired with geophone arrays at 5, 10, 20, and 40 m spacing. One of the more striking results from that work was the observation that

abundant coherent noise isn't even visible on the gathers with the larger spacing, although it's clearly present on the more finely sampled gathers. Noise can only be removed if it can be observed and characterized accurately.

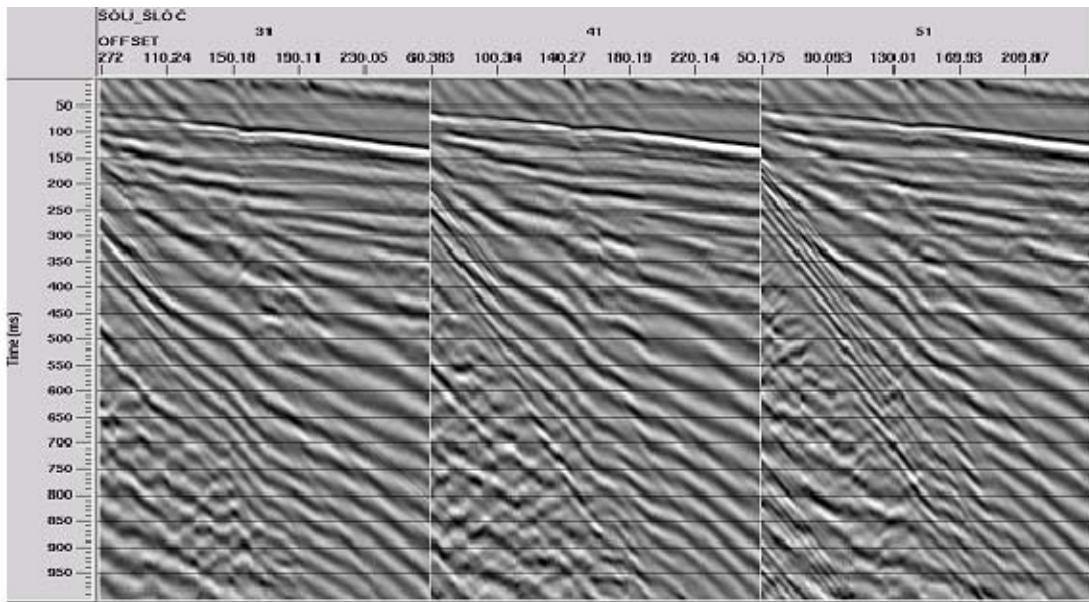
Although the bulk of the coherent noise on the Longview experiment was captured and removed with the 2.5 m station spacing, we could observe some aliasing, particularly for the slowest noises at or below air velocity. Thus, we decided to reduce the sampling interval even more; and in March 2008, we conducted a small survey at the University of Calgary Priddis test site in which the surface sampling was 1 m. Unlike the Longview experiment, we used 3C geophones so that we could examine the resolution issue for horizontal seismic components, as well as vertical. In addition to the 200 m long fixed spread of 3C phones, a 20 m landstreamer with 3C phones spaced at 1m intervals was deployed for comparison (Suarez, 2008). Both the fixed conventional spread and the landstreamer were recorded simultaneously using a source line offset 5 m laterally from the geophone line. The source positions along this line were distributed every 10 m over a distance of 400 m, centred on the geophone line. Thus, source-receiver offsets ranged from 5 m for the geophone closest to the source position to 300 m for the source positions at the extreme ends of the source line. The source for the entire experiment was the U of C mini-vibe, using a sweep range of 5 – 250 Hz. Since the landstreamer was so short (20 m) and required nine position changes in order to cover the same ground as the 200 m fixed spread, the vibrator repeated each source position ten times. In her comparison study, Suarez (2008) used a subset of the complete fixed spread survey (one tenth of it) to compare with the landstreamer results. Here, however, we employ vertical stacking to composite all ten basically identical shot records recorded into the fixed spread for each source position.

PROCESSING

The vertical component

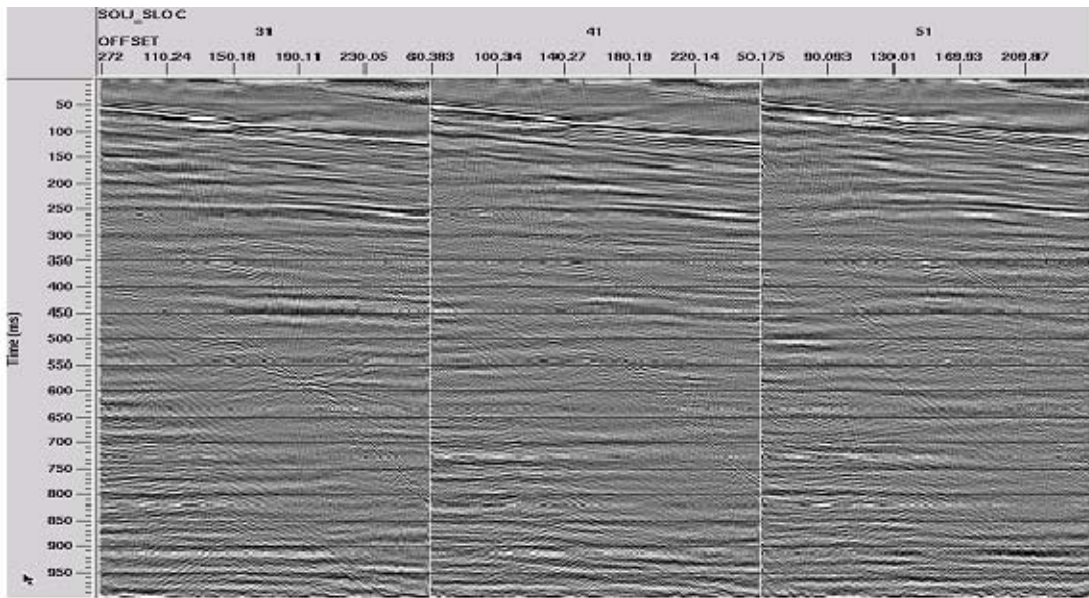
Our procedure for processing the Priddis data was similar to that used with the Longview experiment as reported in 2006. As in the Longview example, the shot gathers for the data sets were processed for noise attenuation by analyzing and removing the noises which could be unambiguously characterized on the displays of the gathers. Deconvolution, and NMO correction were applied to the gathers prior to CDP stacking; , followed by post-stack Kirchhoff migration or residual noise attenuation to bring the data to their final resolution. In the case of the two horizontal components, rotation of these raw components were required before further processing, since the source positions were laterally offset from the geophone spread by 5 m, which is five times the basic station interval, and thus not insignificant.

Figure 1 shows a group of three vertical component shot gathers from near the beginning of the line. As is typical of high resolution data from this general region, no reflections are visible on the raw records. Figure 2 shows the same shot records after several radial trace filter passes, followed by Gabor deconvolution. Reflections are now readily visible, but the shallower reflections (around 250 ms) are observed mainly on the longest offset traces. This may mean that the low velocity coherent noise formerly contaminating these records was so strong that little signal remains when the noise is removed.



Raw vertical component shot gathers from Priddis 1m survey

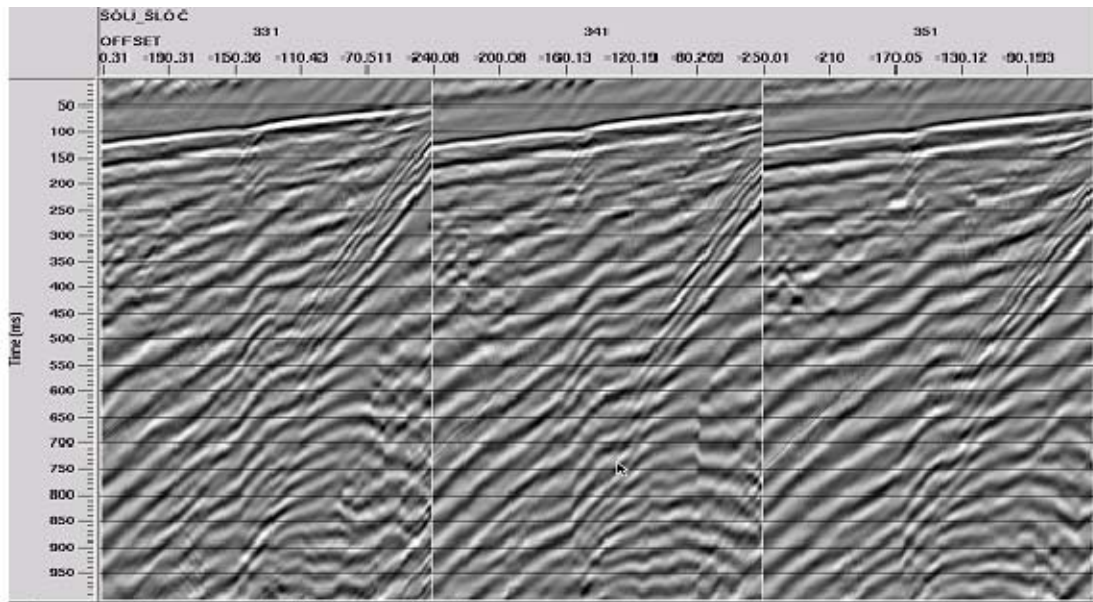
FIG. 1. Raw vertical component shot gathers before any processing. Only coherent noise and backscatter are visible on the records. No aliasing is apparent.



Typical vertical component gathers from the Priddis 1m survey, after filtering and deconvolution

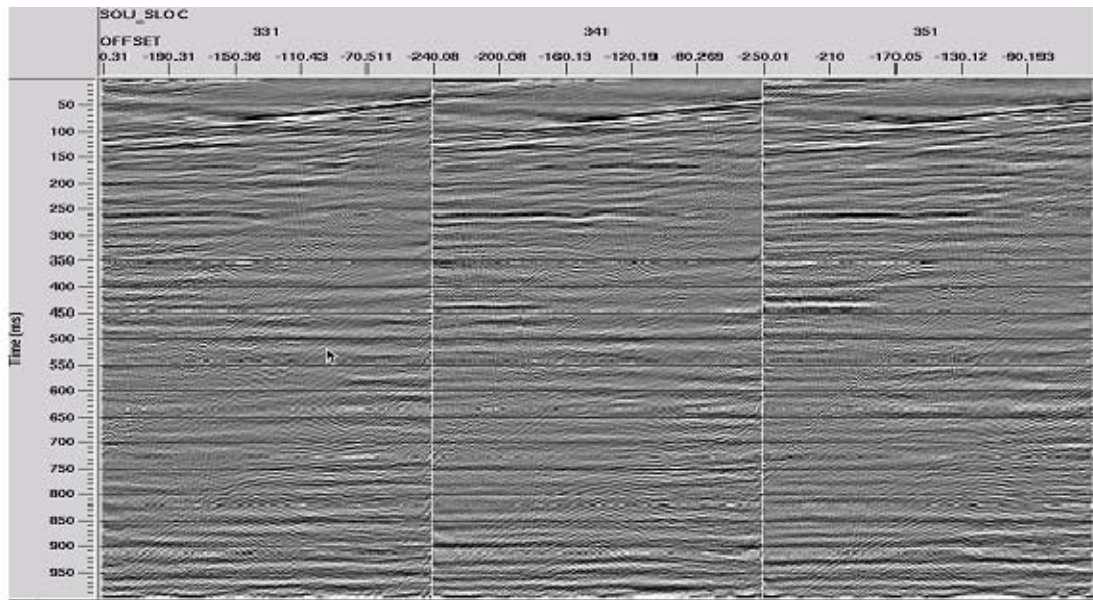
FIG. 2. Vertical component gathers from Figure 1 after coherent noise attenuation and deconvolution. The reflections at 250 ms are mainly visible at the longer offsets.

Figures 3 and 4 show three shots from the opposite (east) end of the line, in their raw, and processed forms, respectively. As with the previous displays, no reflections can be seen on the raw records in Figure 3. The 250 ms reflection on the processed records extends across most of the offsets, however, indicating a better S/N on this end of the line,



Typical vertical component shot gathers from Priddis 1m survey

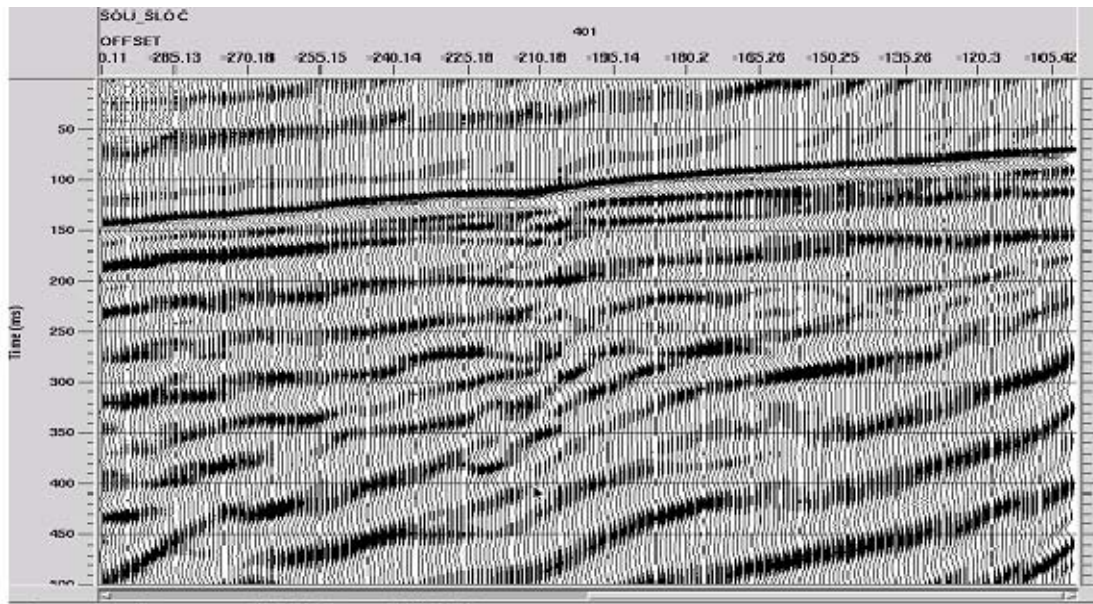
FIG. 3. More vertical component shot gathers from the other end of the Priddis 1 m survey. No reflections are visible, but noise appears well-sampled.



Typical vertical component shot gathers from Priddis 1m survey, after filtering and deconv

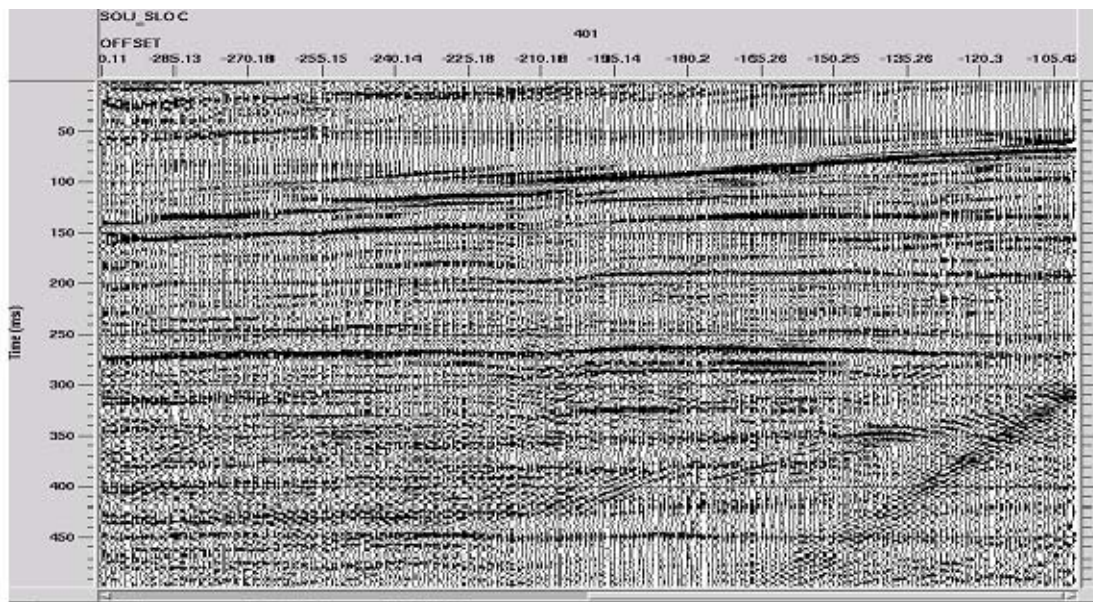
FIG. 4. Vertical component shot gathers from Figure 3 after coherent noise attenuation and deconvolution. Reflections are now visible. Reflection at 250 ms is mostly visible at the longer offsets.

Figures 5, 6, 7, and 8 show one shot record on the high numbered end of the line in more detail. We use wiggle trace for Figures 5 and 6 and variable density for Figures 7 and 8, just to show different characteristics of the same data.



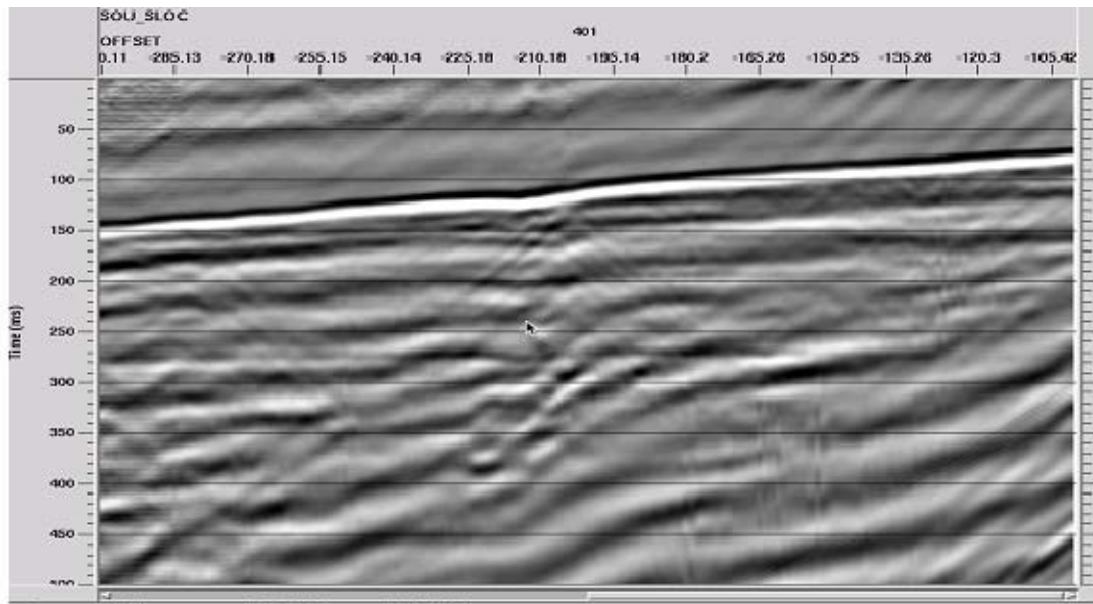
Long offset vertical component shot gather from Priddis 1m survey

FIG. 5. Long offset vertical component from Priddis survey. Note the linear arrival radiating at air velocity from the ground depression in the middle of the record.



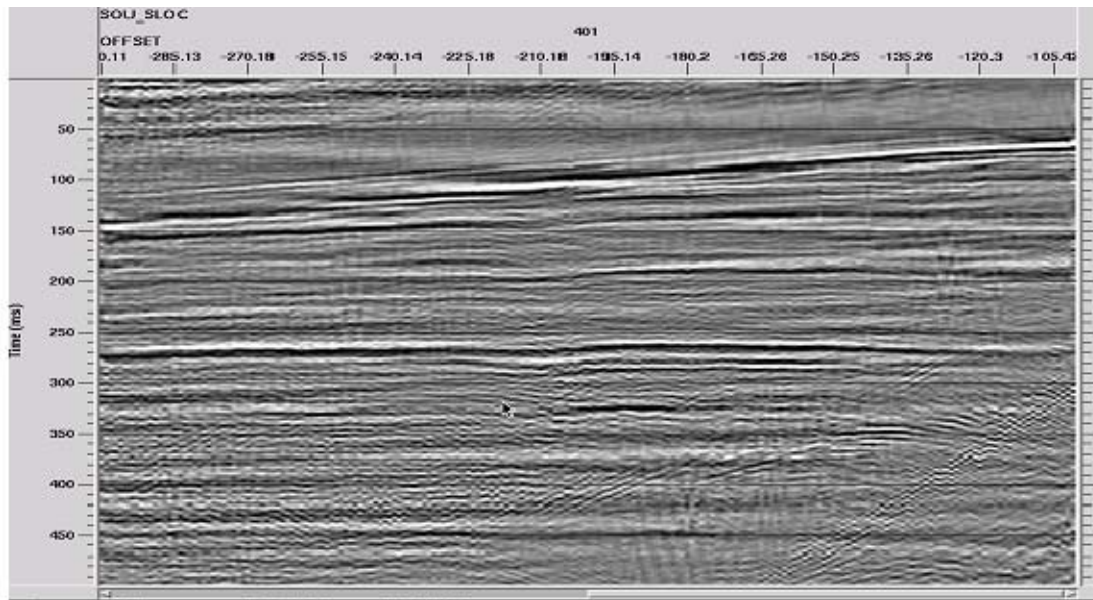
Long offset vertical component shot gather from Priddis 1m survey, after filtering and deconvolution

FIG. 6. Long offset vertical component record after coherent noise attenuation and deconvolution. Some noise aliasing is visible after deconvolution.



Long offset vertical component shot gather from 1m Priddis survey

FIG. 7. Long offset raw vertical component record displayed in variable density. Note the linear noise radiating away from the surface depression.



Long offset vertical component shot gather from Priddis 1m survey, after filtering and deconvolution

FIG. 8. Long offset vertical component gather after coherent noise attenuation and deconvolution.

It is interesting to note the presence of a linear noise on this gather, radiating from a slight irregularity in the surface of the earth, at the velocity of sound in air. On the wiggle trace gather in Figure 5, the noise appears to radiate mainly away from the source, while the variable density gather in Figure 7 shows some slight radiation in the backward direction, as well. The radial trace filtering and deconvolution operations appear to have attenuated this noise and others almost completely.

The gathers for this line showed little evidence of statics, so we chose to ignore statics and to simply image the data in their current form. As a basis for judging the effectiveness of our pre-stack processing, we present in Figure 9 the “brute” stack of all the source gathers, with no pre-stack noise attenuation or deconvolution. We have applied only a post-stack whitening deconvolution, followed by a zero phase bandpass for display purposes.

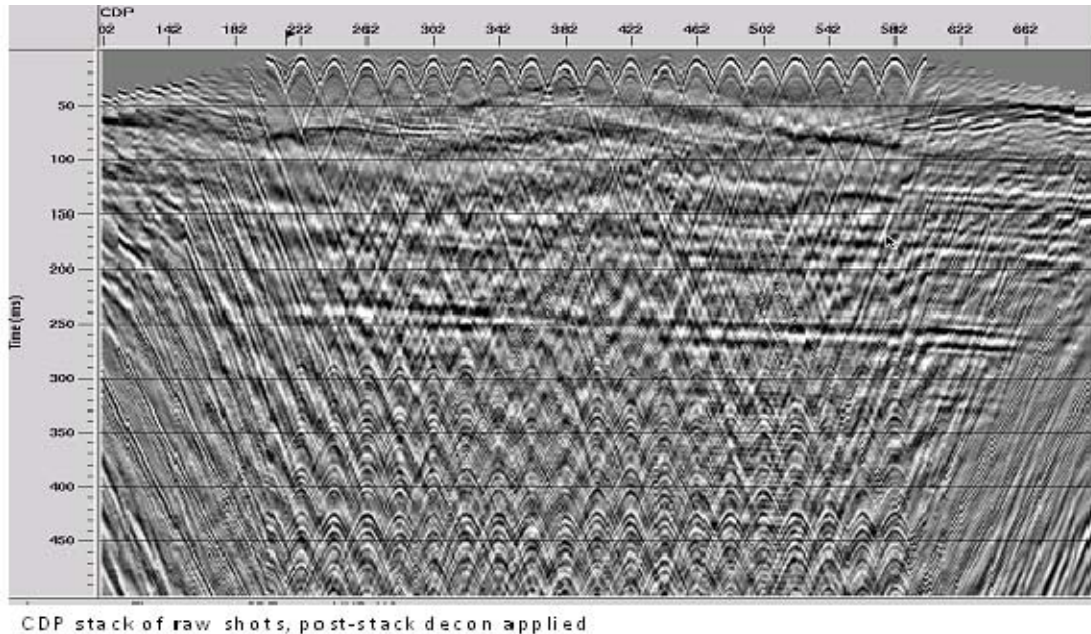
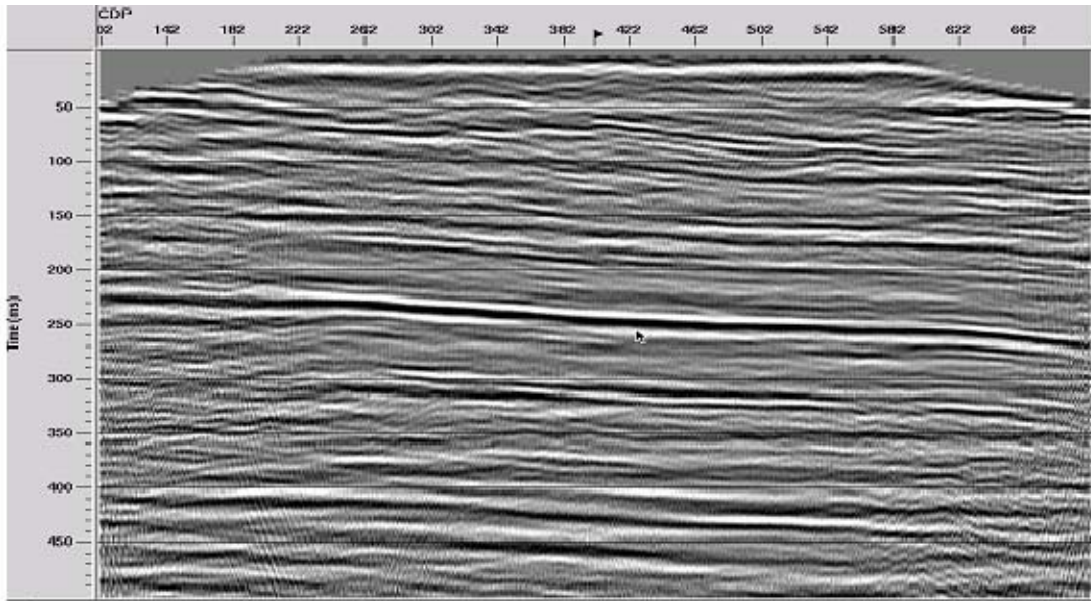


FIG. 9. CDP stack of raw shots, with post-stack Gabor whitening deconvolution and a zero phase bandpass filter applied for display purposes. We thus confirm the presence of reflections down to at least 500 ms, though they are badly obscured by coherent noise.

Since the offsets on this line are so small, stacking velocity need not be determined with great accuracy. Almost anything between 2000 and 3000 m/s will stack all the events on the section. Nevertheless, we attempted to refine velocities above ~250 ms to retain as much of the flat part of each reflection event as possible within the constraints of stretch muting applied by the NMO operation.

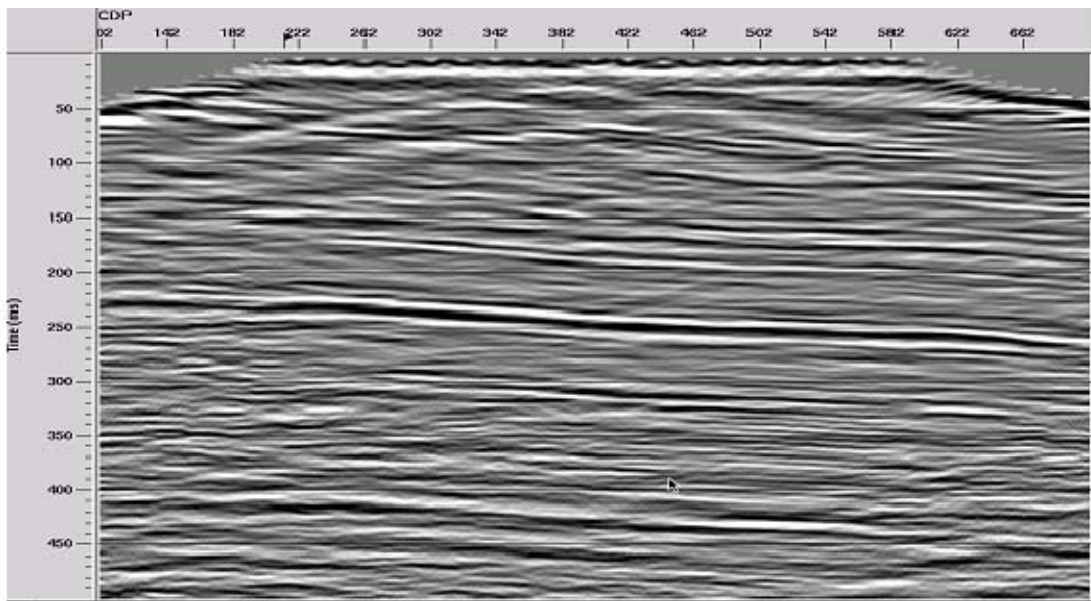
When we attenuate linear noises on the raw records to the best of our ability, apply Gabor deconvolution, stack with the same velocity function as in Figure 9, do some post-stack radial trace filtering for residual coherent noise, and apply fx-decon for random noise attenuation, we obtain the section in Figure 10. We can easily find the prominent events in Figure 9 on the improved stack in Figure 10, as well as many others which were previously obscured. To be objective, post-stack radial filtering and fx-decon would certainly improve the stack in Figure 9, as well, but the signal bandwidth would not be as broad as we observe in Figure 10. To illustrate another way of processing these data, we present also Figure 11, in which the filtered, deconvolved pre-stack data are migrated post-stack with Kirchhoff time migration. In this case, we apply the same post-stack whitening deconvolution with the Gabor algorithm, but we do not apply radial filtering or fx-decon, since the migration accomplishes much of the noise attenuation. Figure 11 is

not greatly different in detail from Figure 10, but the deeper events seem better resolved in Figure 11 and the shallower events better resolved in Figure 10.



CDP stack of filtered, deconvolved shots. Post-stack filtering, decon, fx-decon applied

FIG. 10. Best CDP stack obtained with shots which have been filtered for coherent noise and deconvolved with Gabor deconvolution. The stack has been filtered for residual coherent and random noise and has been whitened with Gabor deconvolution.



CDP stack of vertical component shots, post-stack decon, post-stack time migration

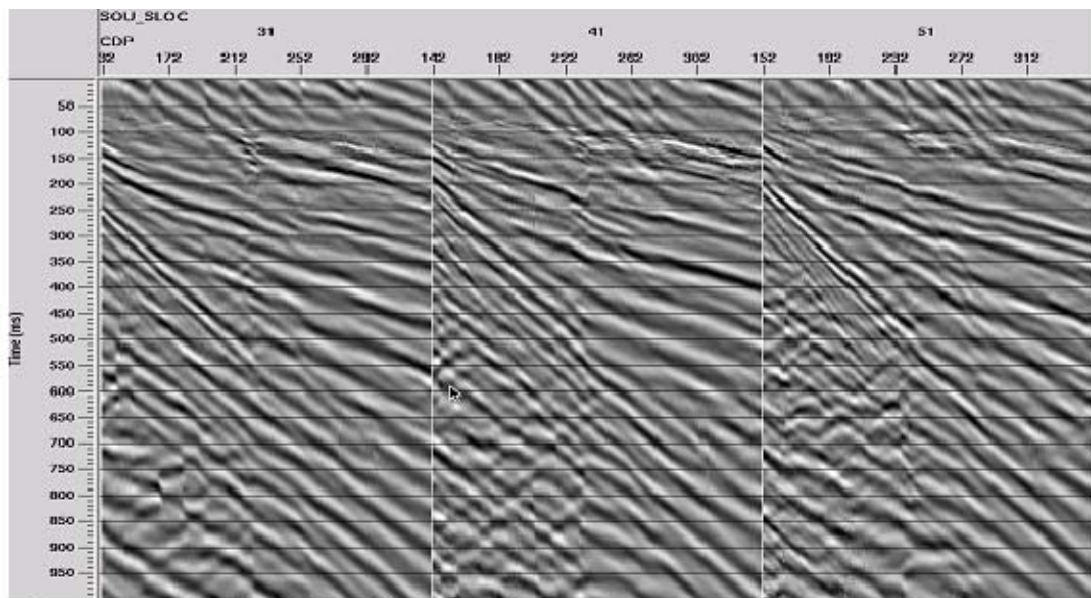
FIG. 11. CDP stack with Kirchhoff time migration applied, rather than post-stack coherent and random noise attenuation. The whitening deconvolution is the same as applied for Figures 9 and 10. The deeper events seem to have more detail in this section, but the shallow events seem less well resolved.

The sections in Figures 9, 10, and 11 confirm what we know about the near-surface geology in the Priddis region—shallow reflections correspond to sediments with a gentle east dip which sub-crop against the weathered layer. The sections also confirm that even though our raw records are exceedingly noisy, we can obtain acceptable images from them because we have sampled the pertinent coherent noises well enough to characterize them and remove them.

The horizontal components

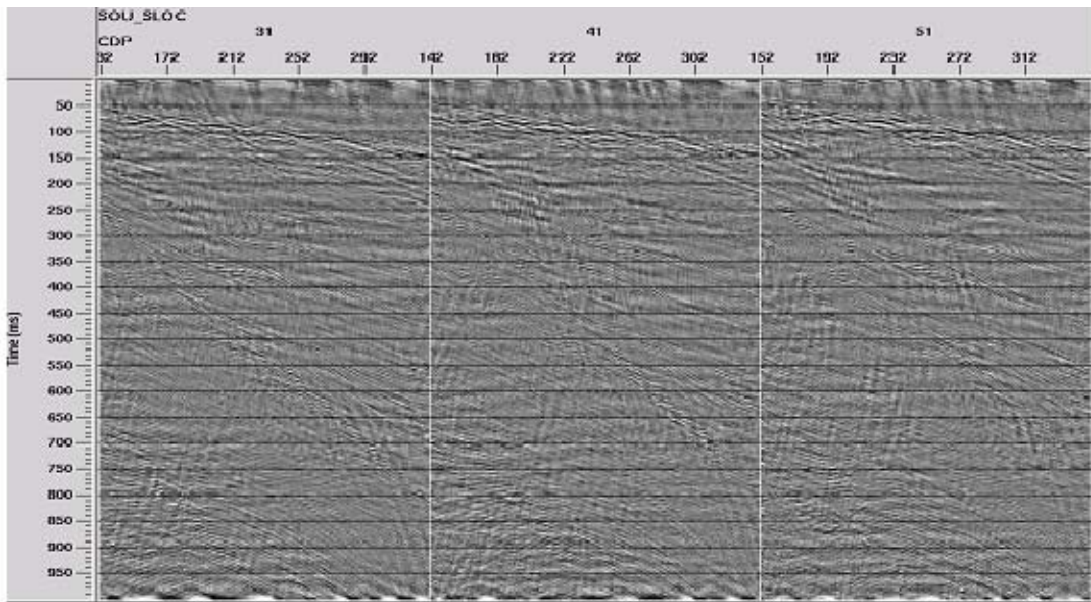
Since this is a 3C line, we processed the horizontal components as well, although we did not particularly expect to find converted wave responses for any but the very shallowest of layers, since the source-receiver offsets for the line were likely inadequate to provide the proper aperture for P-S mode conversion.

Since the source positions were offset laterally from the receiver line, The horizontal component recorded as 'inline' would contain varying amounts of 'xline' energy, particularly in the geophones with the shortest source-receiver offsets, and vice-versa. This makes it necessary to rotate the two components prior to further processing, in order to obtain source gathers which correspond to energy radiating directly away from the source and gathers whose energy is truly transverse to the source direction. Figure 12 shows 3 raw long-offset source gathers which have been rotated to the true 'inline' (radial) direction, while Figure 13 shows the same gathers after our best effort at coherent noise attenuation and deconvolution. In contrast to the vertical component gathers in Figures 2 and 4, there is little to see in these gathers in the way of coherent reflected or converted wave events. About all we can see is a low level background of residual linear noise and a couple of shallow fragments of events at about 150 ms.



Typical horizontal component gathers after rotation to 'inline' direction

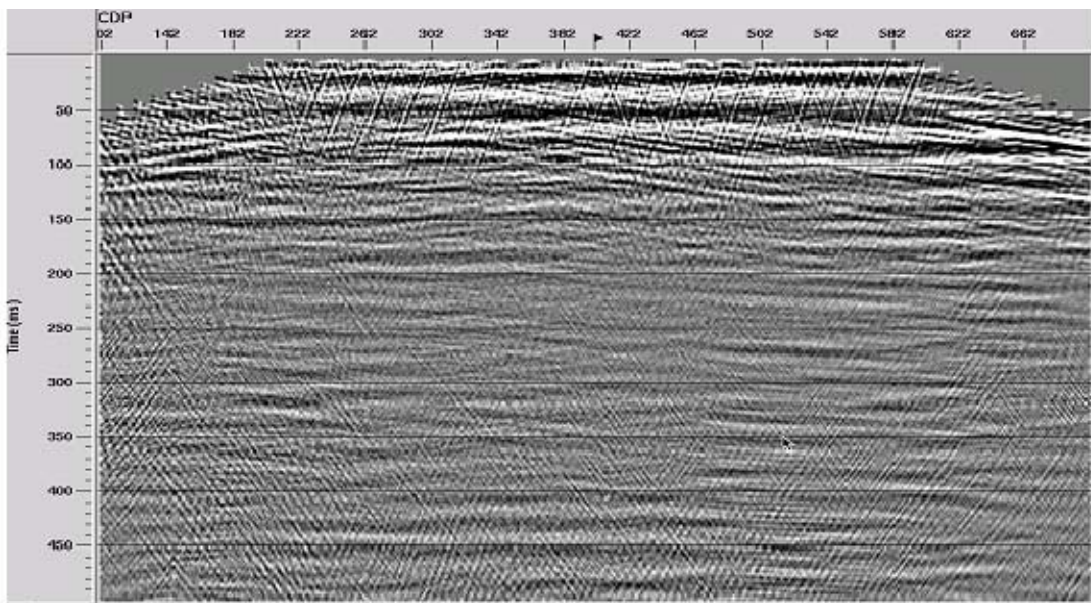
FIG. 12. Long-offset source gathers after rotation to the 'inline' (radial) direction. Linear noise is about all that's visible on these records.



Inline horizontal component gathers after filtering and decon

FIG. 13. Long-offset source gathers after rotation to the 'inline' (radial) direction and after attenuation of coherent noise and Gabor deconvolution. There is little energy on any of these gathers that resembles reflected or converted energy.

With no particular events to analyze for velocity, we made two attempts at stacking these gathers—one, a CDP stack using the stacking velocities of the vertical component, and two, an approximate CCP stack.



CDP stack of rotated inline component ... vertical component velocities

FIG. 14. CDP stack of rotated, filtered, deconvolved 'inline' (radial) component. The dipping events at around 100 ms are almost certainly leakage from the vertical component.

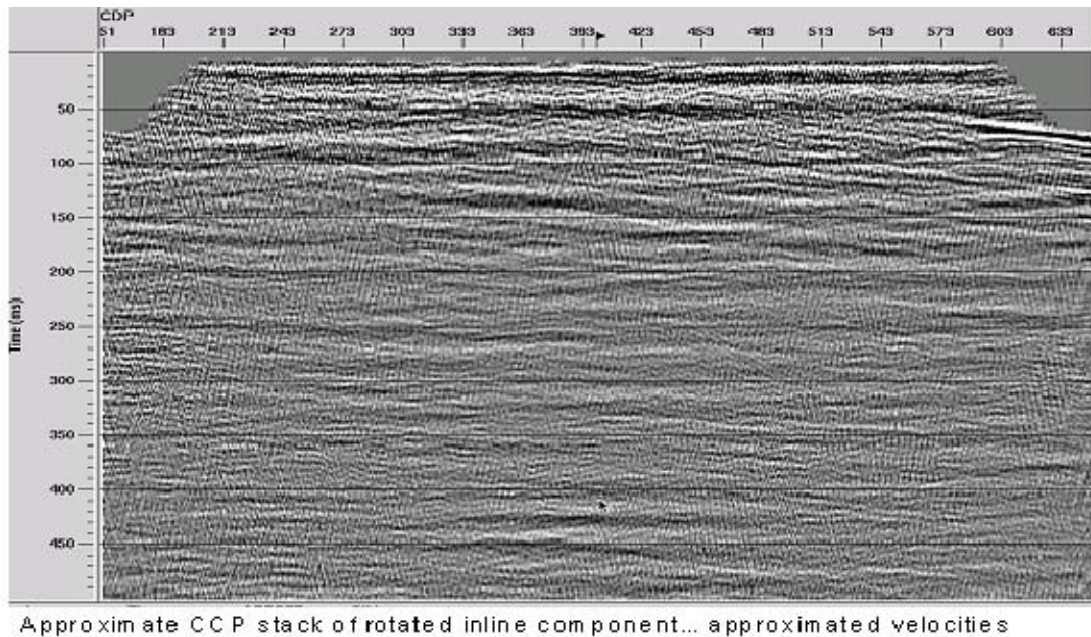
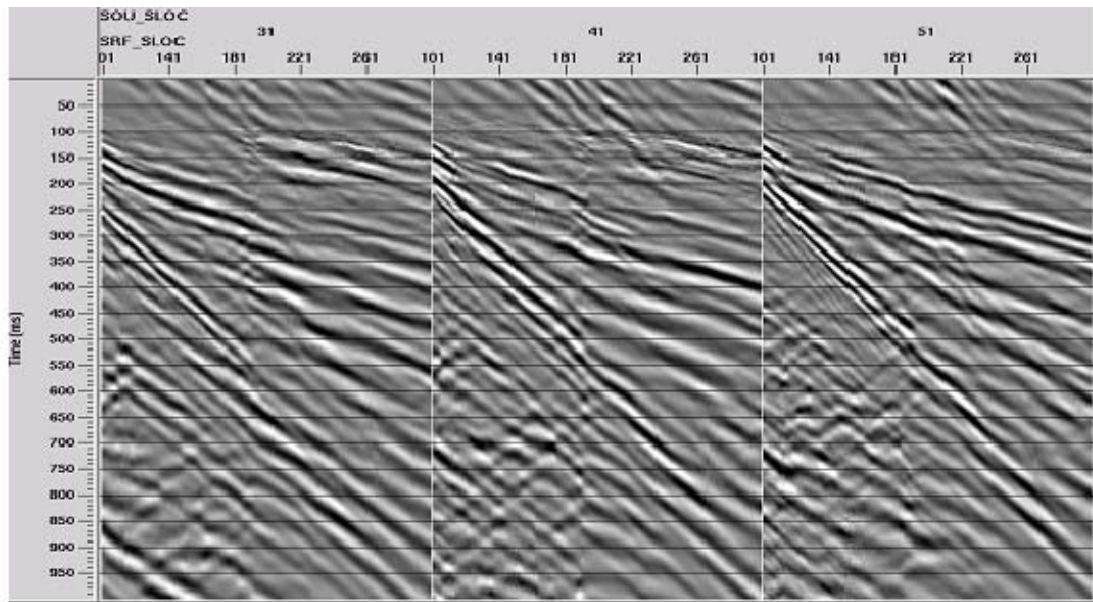


FIG. 15. Approximate CCP stack of rotated, filtered, deconvolved 'inline' (radial) component. The CCP was approximated by $2/3$ the offset from source to receiver, the moveout velocities approximated by $2/3$ the vertical stacking velocities.

The approximate CCP stack is created by assigning a nominal conversion point for each trace, corresponding to an assumed V_p/V_s ratio. In this case, we simply assumed that for any shallow horizons likely to generate converted waves the conversion point would lie approximately $2/3$ of the distance from source to receiver, rather than $1/2$ of the distance for a common reflection point (CRP or CDP). For each trace in a gather, we replaced the CDP trace header with the estimated CCP. As a further approximation, we applied NMO using $2/3$ of the vertical stacking velocity function. Figure 14 shows the CDP stack of the 'inline' (radial) component, while Figure 15 shows the approximate CCP stack. It would be hard to make a case for any particular converted wave events on either of these sections. The dipping events toward the right on both sections are likely leakage from the vertical component.

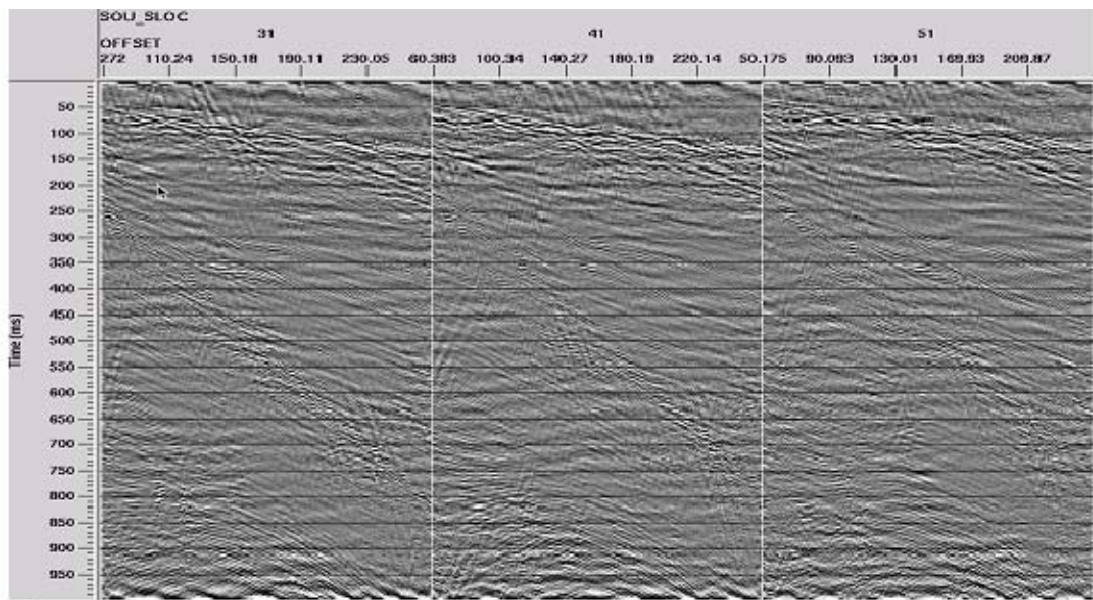
Figure 16 shows three long-offset raw horizontal component records after being rotated to the 'xline' (transverse) direction, and Figure 17 shows them processed in the same manner as the 'inline' shots. The result of noise attenuation and deconvolution on these gathers is much the same as for the 'inline' gathers—there is little coherent energy on these records that could be converted waves.

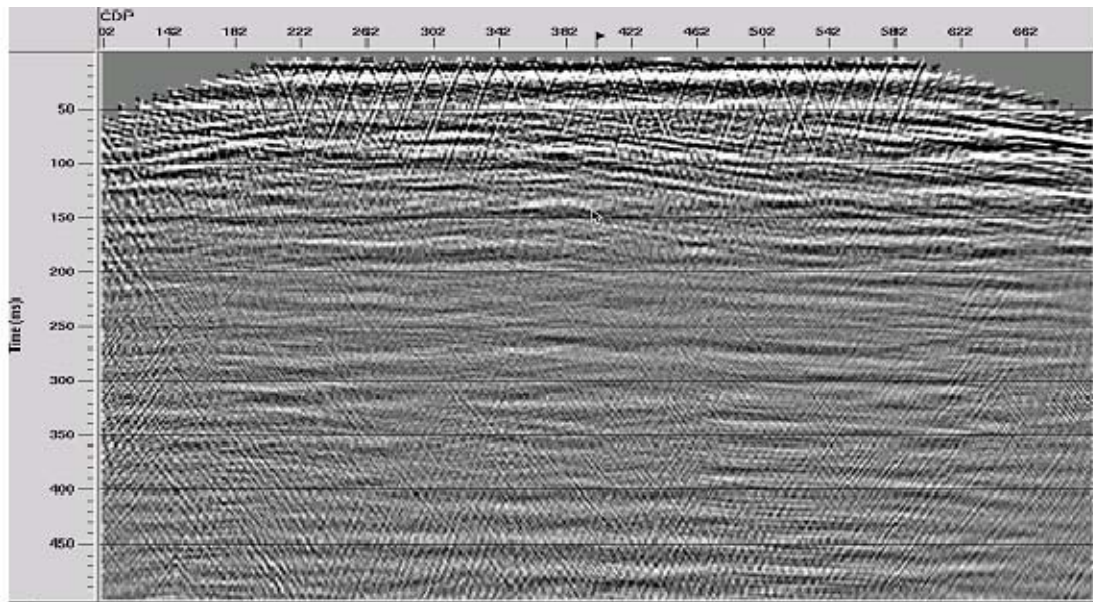
Figures 18 and 19 show the CDP stack and approximate CCP stack for the 'xline' (transverse) gathers. Other than some leakage of vertical component, no events on either section appear to be legitimate converted wave events.



Typical horizontal component gathers after rotation to 'xline' direction

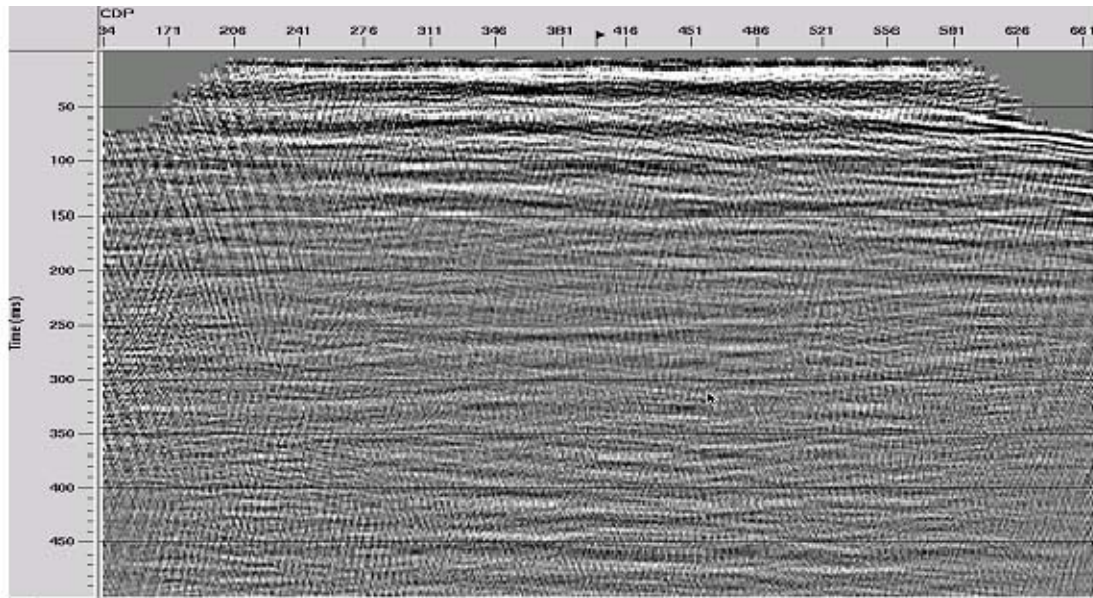
FIG. 16. Long-offset horizontal component gathers after rotation to the 'xline' (transverse) direction. Only coherent noise is visible on these gathers.





CDP stack of rotated 'xline' component... vertical component velocities

FIG. 18. CDP stack of rotated 'xline' (transverse) horizontal component using vertical component velocities. Dipping events are likely leakage from the vertical component, as well as unfiltered noise residuals.



Approximate CCP stack of rotated 'xline' component... approximate velocities

FIG. 19. Approximate CCP stack of rotated 'xline' (transverse) horizontal component using $2/3$ times the vertical stacking velocities. No events on this section appear to be legitimate converted wave events.

For this experiment, the horizontal components appear to bear little coherent energy from converted waves. This is likely due to the very limited aperture imposed by the very short length of the line.

CONCLUSIONS

The field experiment at the Priddis site had several research objectives, only one of which is addressed here—that of exploring the limits of high resolution acquisition. A previous experiment near Longview had shown us that the more closely spaced the geophones, the smaller the chance of aliasing coherent noise generated by the seismic source, and the higher the resolution of the resulting images. Even on those data, however, with their 2.5 m geophone spacing, some aliasing was observed for the highest frequencies at the slowest apparent velocities. The intent of the Priddis experiment was to extend the resolution even further by reducing the phone spacing to 1 m. Unfortunately, a constraint on available equipment limited the total length of the spread, and thus the range of source-receiver offsets recorded. Nevertheless, using the same processing and analysis procedures as for the Longview experiment, we have obtained some very acceptable reflection images from the vertical component of the data set. The quality of these images was shown to be directly dependent upon the pre-stack coherent noise attenuation applied to the gathers, which was, in turn, enabled by the proper sampling of the coherent noise modes by the 1 m geophone spacing. Unlike the Longview data set, whose structural flatness raised suspicion about the reality of the reflection events imaged, the reflection events at Priddis exhibit a structural dip (cf. Lu et al., 2008), which proves their reality.

Since we were unable to identify any converted wave events, we can't make the case that 1 m spatial sampling helps for imaging them; but we can note that the coherent noise attenuation enabled by the spatial sampling reveals fairly convincingly that there really are no coherent seismic events hiding behind the noise.

ACKNOWLEDGEMENTS

The authors wish to acknowledge the assistance in the field of Peter Manning, Rolf Maier, Joe Wong, Gabriela Suarez, and Alejandro Alcudia. We also acknowledge the ongoing support of CREWES sponsors.

REFERENCES

- Henley, D.C., Bertram, M., Hall, K., Bland, H., Gallant, E., and Margrave, G.F., 2006, The power of high effort seismic acquisition: the Longview experiment: CREWES 2006 Research Report, **18**.
- Lu, H., Hall, K.W., Lawton, D.C., and Stewart, R.R., 2008, Processing the Priddis 2007 geophysics field school 3D survey: CREWES Research Report, **20**.
- Suarez, G., 2008, Side-by-side comparison of 3C land streamer versus planted geophone data at the Priddis test site: CREWES Research Report, **20**.